View metadata, citation and similar papers at core.ac.uk

brought to you by CORE

provided by Elsevier - Publisher Connector

Scientia Iranica B (2011) 18 (6), 1231–1236

Sharif University of Technology

Scientia Iranica

Transactions B: Mechanical Engineering

www.sciencedirect.com

Effect of specific heat ratio on heat release analysis in a spark ignition engine

R. Ebrahimi

Department of Agriculture Machine Mechanics, Shahrekord University, Shahrekord, P.O. Box 115, Iran

Received 25 July 2010; revised 8 July 2011; accepted 6 September 2011

KEYWORDS

Spark ignition engine;
Specific heat ratio;
Combustion parameters;
Heat release rate;
Natural gas operation;
Gasoline operation.

Abstract The specific heat ratio used in heat release calculations plays a crucial role in the determination of combustion parameters. In this study, the effects of assumed specific heat ratio on the heat release analysis of engine pressure data are studied in a spark ignition engine, using natural gas and gasoline fuels. The experiments were carried out with the spark timing adjusted to the maximum brake torque timing, at an equivalence ratio of $\phi = 1$ and a speed engine of $N = 3300$ rpm. The combustion parameters are obtained from the heat release rate, which obtained from the first law of thermodynamics during a cycle. The results show that the combustion parameters have high sensitivity to the variation and first derivative of the specific heat ratio. The results also show that the influence of the first derivative of the specific heat ratio on the combustion parameters for natural gas operation is higher than that for gasoline operation. Moreover, the first derivative of the specific heat ratio for determination of combustion parameters should not be ignored.

© 2012 Sharif University of Technology. Production and hosting by Elsevier B.V.
Open access under CC BY license.

1. Introduction

Cylinder pressure measurements in thermodynamics analysis are clearly a useful tool for calculating combustion parameters. In other words, cylinder pressure directly gives work production in the combustion chamber, and thus gives an important insight into the control and tuning of the engine [1,2]. The calculation of the Heat Release Rate (HRR) is obtained from the first law of thermodynamics during a cycle. It can be applied as a useful tool for calculation of the principal combustion characteristics [3,4]. The specific heat ratio is the most important thermodynamic property used in heat release analysis, since the specific heat ratio couples system energy to other thermodynamic quantities. Many previous studies towards the effect and calculation of specific heat ratio in the first law heat release model have been carried out. Abu-Nada et al. [5] studied the thermodynamics analysis of a spark ignition engine. It was resulted that engine working parameters were affected by variable specific heats. The results also showed that the temperature dependent on the specific heat of the working fluid had an impact on the performance of the Otto cycle. Klein and Eriksson [6] found a specific heat ratio model during the combustion process, using the Mass Fraction Burned (MFB). Lanzafame and Messina [7] estimated the influence of gas thermodynamic properties on gross heat release. Brunt et al. [8] showed that the calculated gross heat release is highly dependent on the assumed values for the specific heat ratio and the charge to wall heat transfer. Chun and Heywood [9] proposed a linear function of the mean charge temperature for a specific heat ratio, e.g. $\gamma = a + bT$. The constants, a and b, were determined for each fuel and equivalence ratio. Figure 1 shows the specific heat ratio versus temperature for natural gas and gasoline fuels at an equivalence ratio of $\phi = 1$, according to the methodology proposed by Chun and Heywood [9]. The slope of the specific heat ratio versus temperature for natural gas fuel is higher than that of gasoline fuel. It also reveals that the value of the specific heat ratio for natural gas is higher than that for gasoline, when the temperature is less than 1530 K. While, after this critical temperature, the specific heat ratio for natural gas fuel is less than that for gasoline fuel.

Comparative studies of the effects of variation and the first derivative of specific heat ratio on combustion parameters

E-mail address: Rahim.Ebrahimi@gmail.com.

1026-3098 © 2012 Sharif University of Technology. Production and hosting by Elsevier B.V. Open access under CC BY license.

Peer review under responsibility of Sharif University of Technology.

doi:10.1016/j.scient.2011.11.002

Production and hosting by Elsevier

Nomenclature

A	wall area, m^2
B	cylinder bore diameter, m
c_v	specific heat at constant volume, J kg^{-1} K^{-1}
h	heat transfer coefficient for gases in the cylinder, W m^{-2} K^{-1}
m	charge mass, kg
m_f	mass of fuel, kg
N	engine speed, rpm
p	cylinder gas pressure, Pa
Q_{ch}	chemical energy release by combustion, J
Q_{ht}	heat transfer to the chamber walls, J
Q_{LHV}	lower heating value
R	gas constant, J kg^{-1} K^{-1}
T	mean gas temperature, K
T_W	wall temperature, K
V	cylinder volume, m^3

Greek symbols

ϕ	equivalence ratio
γ	specific heat ratio
θ	crank angle, degree

Abbreviations

CHR	Cumulative Heat Release
CHR_{max}	Maximum Cumulative Heat Release
HRR	Heat Release Rate
HRR_{max}	Maximum Heat Release Rate
IVC	Intake Valve Close
IVO	Intake Valve Open
MBT	Maximum Brake Torque
MFB	Mass Fraction Burned
SD	Standard Deviation
WOT	Wide Open Throttle

for gasoline and natural gas operations in a spark ignition engine do not appear to have been published. Therefore, in this study, the effects of assumed specific heat ratio on the heat release analysis of engine pressure data are studied by applying the first law of thermodynamics to the cylinder charge in a spark ignition engine for natural gas and gasoline fuels. The parameters chosen are HRR, maximum HRR (HRR_{max}), division of HRR by its maximum (HRR/HRR_{max}), Cumulative Heat Release (CHR) and 10% and 90% Mass Fraction Burned Position (MFBP).

2. Experimental analysis

The experimental system is shown in Figure 2. In the experimental study, the spark ignition engine was modified to operate with gasoline and natural gas fuels. Details of the engine specification are shown in Table 1. The cylinder pressure measurement was taken by means of a Kistler 6055B glow-plug piezoelectric transducer. For each measuring point, the pressure data of 100 consecutive cycles were sampled and recorded. Before the calculation of the apparent heat release rate, the ensemble averaged pressure data were smoothed with a Fourier series high-frequency-reject filtering algorithm, which used a Gaussian roll-off function [10].

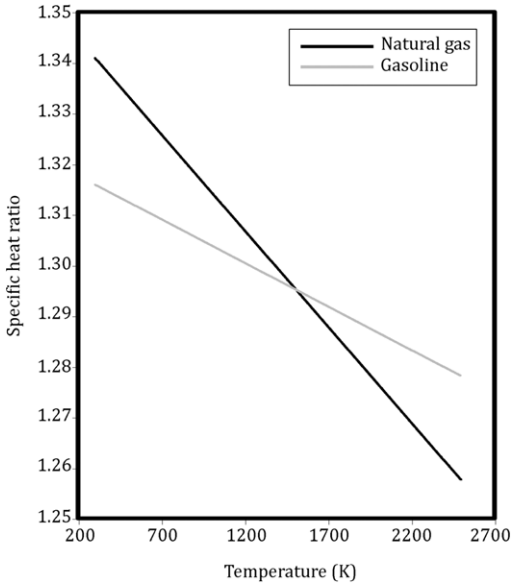

Figure 1: Specific heat ratio for natural gas and gasoline fuels versus temperature for a equivalence ratio of $\phi = 1$, according to the methodology proposed by Chun and Heywood [9].

Table 1: Specifications of test engine.

Cylinder bore	76 mm
Piston stroke	87 mm
Length of connecting rod	148 mm
Compression ratio	9.6

Table 2: Accuracies of the measurements and the uncertainties in the calculated results.

Parameter	Accuracy	Percentage uncertainties
Pressure pick up	±1 bar	±0.1
Speed measuring unit	±10 rpm	±0.1
Air flow meter	±0.1 m/s	±0.1
Fuel consumption	±37 g/h	±0.16
Crank angle encoder	±0.2°	±0.15

3. Error analysis

Table 2 shows the accuracies of the measurements and the uncertainties in the calculations. Errors and uncertainties in the experiments can arise from instrument selection, instrument condition, instrument calibration, environment, observation, reading and test planning. Uncertainty analysis was needed to prove the accuracy of the experiments [11]. However, it should be mentioned here that the standard error in measured parameters, such as pressure, and calculated parameters like heat release rate include both the processing uncertainties and cycle-to-cycle fluctuations.

4. Determination of specific heat ratio

The specific heat ratio during the closed part of the cycle is most frequently modelled as either a constant, or as a polynomial function of temperature [2]. In this work, based on assumptions of chemical equilibrium for the burned mixture and frozen mixture for the unburned mixture, the specific heat ratio is calculated. The ranges of temperature were 300–1000 K and 300–2500 K for the unburned and burned mixtures [2]. The

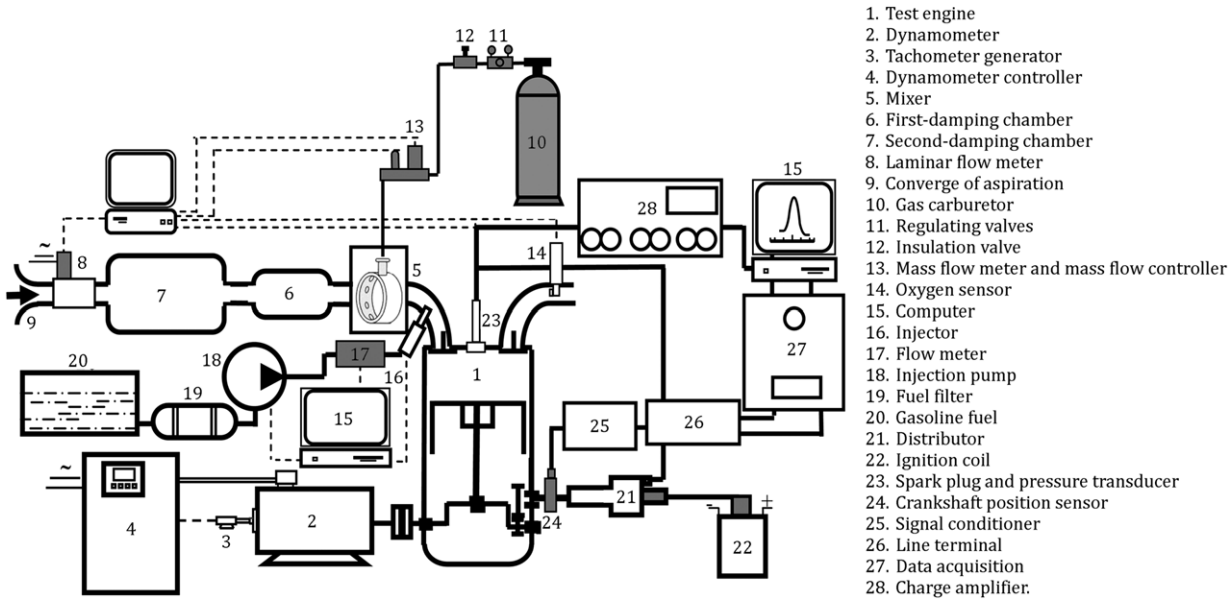

Figure 2: Experimental schematic.

value of the specific heat ratio was used to derive a function for the burned and unburned mixtures, using a least squares approach.

4.1. Equilibrium combustion model

Composition of the combustion products was calculated according to the solution given by Ferguson [12]. At lower temperatures and carbon-to-oxygen ratios less than one, the overall combustion reaction can be represented as [13]:

$$C_aH_b + \frac{a + b/4}{\phi}(O_2 + 3.774N_2) \rightarrow n_1CO_2 + n_2H_2O + n_3N_2 + n_4O_2 + n_5CO + n_6H_2, \quad (1)$$

where ϕ is the equivalence ratio.

For lean mixture products at low temperature, it is assumed that there is no product, CO and H_2. In this case, balance equations are sufficient to calculate the product composition, since there are four unknowns and four equations. For rich mixtures, it is assumed that there is no product, O_2. In this case, there are five unknowns, so one needs an additional equation to supplement the four atom balance equations. The equilibrium considerations between the product species, CO_2, H_2O, CO and H_2, is assumed. This reaction is termed the water–gas reaction:

$$CO_2 + H_2 \leftrightarrow H_2O + CO,$$
$$K(T) = \frac{n_1 n_5}{n_1 n_6}. \quad (2)$$

The overall combustion reaction, according to the model of Olikara and Borman, is [14]

$$C_aH_b + \frac{a + b/4}{\phi}(O_2 + 3.774N_2) \rightarrow n_1H + n_2O + n_3N + n_4H_2 + n_5OH + n_6CO + n_7NO + n_8O_2 + n_9H_2O + n_{10}CO_2 + n_{11}N_2. \quad (3)$$

The air–fuel mixture is frozen for $T < 1700$ and is at equilibrium otherwise [13]. Atom balancing yields four equations. Thus, six gas phase equilibrium reactions are introduced, in order to obtain a composition solution. The equilibrium constant data were obtained from [12].

Equilibrium reaction	Equilibrium constant	
$\frac{1}{2}H_2 \overset{(1)}{\longleftrightarrow} H$	$K_1 = \frac{y_1 p^{1/2}}{y_4^{1/2}}$,	(4)
$\frac{1}{2}O_2 \overset{(2)}{\longleftrightarrow} O$	$K_2 = \frac{y_2 p^{1/2}}{y_8^{1/2}}$,	(5)
$\frac{1}{2}N_2 \overset{(3)}{\longleftrightarrow} N$	$K_3 = \frac{y_3 p^{1/2}}{y_{11}^{1/2}}$,	(6)
$\frac{1}{2}H_2 + \frac{1}{2}O_2 \overset{(4)}{\longleftrightarrow} OH$	$K_4 = \frac{y_5}{y_4^{1/2} y_8^{1/2}}$,	(7)
$\frac{1}{2}O_2 + \frac{1}{2}N_2 \overset{(5)}{\longleftrightarrow} NO$	$K_5 = \frac{y_7}{y_8^{1/2} y_{11}^{1/2}}$,	(8)
$H_2 + \frac{1}{2}O_2 \overset{(6)}{\longleftrightarrow} H_2O$	$K_6 = \frac{y_9}{y_8^{1/2} y_4 p^{1/2}}$,	(9)
$CO + \frac{1}{2}O_2 \overset{(7)}{\longleftrightarrow} CO_2$	$K_7 = \frac{y_{10}}{y_6 y_8^{1/2} p^{1/2}}$.	(10)

5. First law heat release rate model

The energy conservation in the cylinder between the inlet valve closure and the exhaust valve closure can be represented as [15]:

$$HRR = \frac{d(mc_vT)}{d\theta} + p\frac{dV}{d\theta} + \frac{dQ_{ht}}{d\theta}, \quad (11)$$

where m is the charge mass, T the mean gas temperature, p the cylinder gas pressure, θ crank angle, c_v the specific heat capacity under constant volume, V the instantaneous volume, and Q_{ht} is the heat transfer to the wall.

For an ideal gas, the equation of state is written as:

$$pV = mRT. \quad (12)$$

Here, R is a gas constant.

Table 3: Different cases of specific heat ratio.

Case	First law heat release rate model	Value of specific heat ratio
1	$\text{HRR} = \frac{\gamma}{\gamma-1}p\frac{dV}{d\theta} + \frac{1}{\gamma-1}V\frac{dp}{d\theta} + \frac{dQ_{ht}}{d\theta}$	$\gamma = 1.25$
2	$\text{HRR} = \frac{\gamma}{\gamma-1}p\frac{dV}{d\theta} + \frac{1}{\gamma-1}V\frac{dp}{d\theta} + \frac{dQ_{ht}}{d\theta}$	$\gamma = 1.3$
3	$\text{HRR} = \frac{\gamma}{\gamma-1}p\frac{dV}{d\theta} + \frac{1}{\gamma-1}V\frac{dp}{d\theta} + \frac{dQ_{ht}}{d\theta}$	$\gamma = 1.35$
4	$\text{HRR} = \frac{\gamma}{\gamma-1}p\frac{dV}{d\theta} + \frac{1}{\gamma-1}V\frac{dp}{d\theta} + \frac{dQ_{ht}}{d\theta}$	According to Section 4
5	$\text{HRR} = \frac{\gamma}{\gamma-1}p\frac{dV}{d\theta} + \frac{1}{\gamma-1}V\frac{dp}{d\theta} - \frac{pV}{(\gamma-1)^2}\frac{d\gamma}{d\theta} + \frac{dQ_{ht}}{d\theta}$	According to Section 4

Variation of gas state equation with crank angle is given by:

$$p\frac{dV}{d\theta} + V\frac{dp}{d\theta} = mR\frac{dT}{d\theta}. \tag{13}$$

The heat release rate can be derived from Eqs. (1) and (3), as given below [16]:

$$\text{HRR} = \frac{\gamma}{\gamma-1}p\frac{dV}{d\theta} + \frac{1}{\gamma-1}V\frac{dp}{d\theta} - \frac{pV}{(\gamma-1)^2}\frac{d\gamma}{d\theta} + \frac{dQ_{ht}}{d\theta}, \tag{14}$$

where γ is the specific heat ratio.

The CHR is obtained from the integral of the HRR curve:

$$\text{CHR} = \int_{\theta=\text{IVO}}^{\theta=\text{IVC}} (\text{HRR})\, d\theta, \tag{15}$$

where IVO is the open intake valve and IVC is the closed intake valve.

The MFB is the normalized integral of the heat release rate:

$$\text{MFB} = \frac{\int_{\theta=\text{IVO}}^{\theta=\text{IVC}} (\text{HRR}) d\theta}{m_f Q_{\text{LHV}}}, \tag{16}$$

where m_f is the mass of fuel and Q_{LHV} is the lower heating value.

The fourth term on the right side of Eq. (14) shows the heat transfer rate between the gas and wall. It is calculated using:

$$\frac{dQ_{ht}}{d\theta} = hA\,(T - T_W)\,\frac{N\pi}{30} = hA\left(\frac{pV}{mR} - T_W\right)\frac{N\pi}{30}. \tag{17}$$

Here, h is the Woschni heat transfer coefficient [17], A is the area in contact with the gas, N is the engine speed, and T_W is the wall temperature.

In order to investigate the effects of specific heat ratio on Eq. (4), five different cases of specific heat ratio are assumed. It should be noted here that the third term on the right side of Eq. (4), $(pV/(\gamma-1)^2)d\gamma/d\theta$, is considered in case 5 and is neglected in cases 1–4. In cases 1–3, the specific heat ratio in Eq. (4) is treated as a constant value; 1.25, 1.3 and 1.35, respectively. In cases 4 and 5, the specific heat ratio is determined based on assumptions of the frozen mixture for the unburned mixture and chemical equilibrium for the burned mixture (see Section 4). The specifications of cases are summarized in Table 3.

6. Results and discussion

The experiments were carried out with the spark timing being adjusted to Maximum Brake Torque (MBT) timing at an equivalence ratio of $\phi = 1$ and a speed engine of $N = 3300$ rpm, for gasoline and natural gas operations.

6.1. Heat release rate

Figure 3 shows the effect of variations in the value of specific heat ratio on HRR for natural gas and gasoline operations. It can be seen that the highest value of HRR_{max} is obtained from case 1 for both fuels, followed by cases 5, 4, 2 and 3 for gasoline operation and by cases 5, 2, 4 and 3 for natural gas operation. Referring to Figure 3, the highest rate of increase in the HRR curve is obtained from case 1, followed by cases 2 and 3, for both fuels. This is due to the fact that the lowest specific heat ratio causes the highest coefficient for pdV and Vdp in Eq. (4). The average SD between HRR values of cases 1–3 from 330 to 420 °CAis 1.9 J/°CA for gasoline operation, and 1.6 J/°CA for natural gas operation. It implies that the sensitivity of the HRR curve to changes in specific heat ratio for gasoline operation is higher than that for natural gas operation. This is due to the fact that the magnitude and rate of increase in HRR for gasoline operation are higher than those for natural gas operation. Conversely, the average SD of HRR between cases 4 and 5 from 330 to 420 °CA is 0.7 J/°CA for natural gas operation, and 1.1 J/ °CA for gasoline operation. This result demonstrates that the HRR curve for natural gas operation is more sensitive to the first derivative of the specific heat ratio, than gasoline operation. This can be attributed to the faster change in the specific heat ratio, due to the rapid change in composition of natural gas fuel during the combustion period, compared to the gasoline operation.

6.2. Cumulative heat release

Figure 4 shows the effect of variations in the value of the specific heat ratio on CHR for both fuels. It can be seen that the specific heat ratio has a very great effect on the magnitude and shape of the CHR curve. The highest value of the maximum cumulative heat release (CHR_{max}) is obtained with case 1 for both fuels, followed by cases 5, 4, 2 and 3 for gasoline operation, and cases 5, 2, 4 and 3 for natural gas operation. When comparing the SD of CHR_{max} between cases 1 and 5 for gasoline operation ($\text{SDCHR}_{\text{max}} = 70.1$ J) and that of natural gas operation ($\text{SDCHR}_{\text{max}} = 67.9$ J), it can be found that the sensitivity of CHR_{max} to changes in specific heat ratio for gasoline operation is higher than that for natural gas operation. The average SD of CHR between cases 1, 2 and 3 from 330 to 420 °CA is about 75.8 J for natural gas operation, and about 83.7 J for gasoline operation. It implies that the sensitivity of the CHR curve to variations in the value of specific heat ratio for gasoline operation is higher than that for natural gas operation. It is also found that the average SD of CHR between cases 4 and 5 from 330 to 420 °CA is about 38.9 J for natural gas operation, and about 25.1 J for gasoline operation. It indicates that the CHR curve for natural gas operation is more sensitive to the first derivative of the specific heat ratio, than that for gasoline operation. By comparing the results obtained from

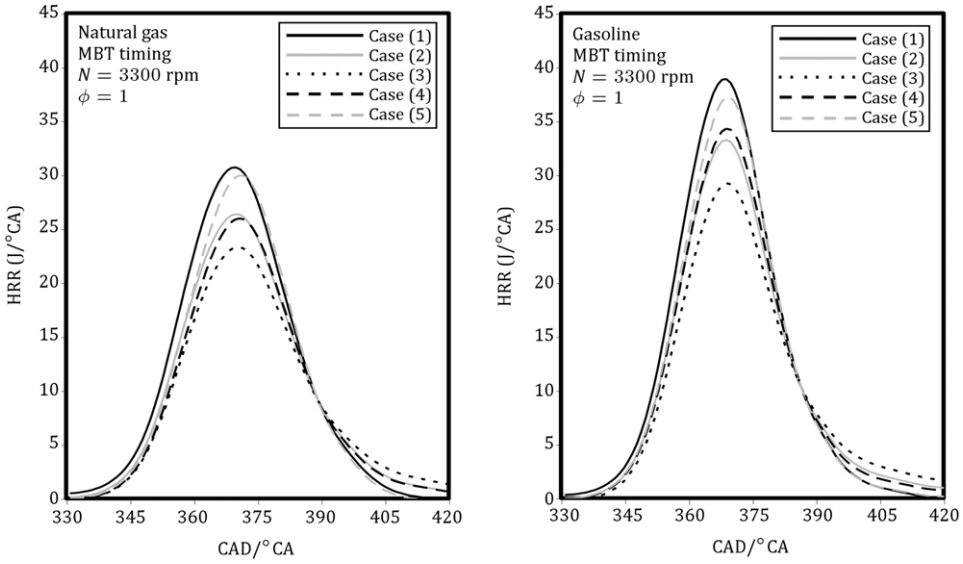

Figure 3: Sensitivity of HRR for cases 1–5.

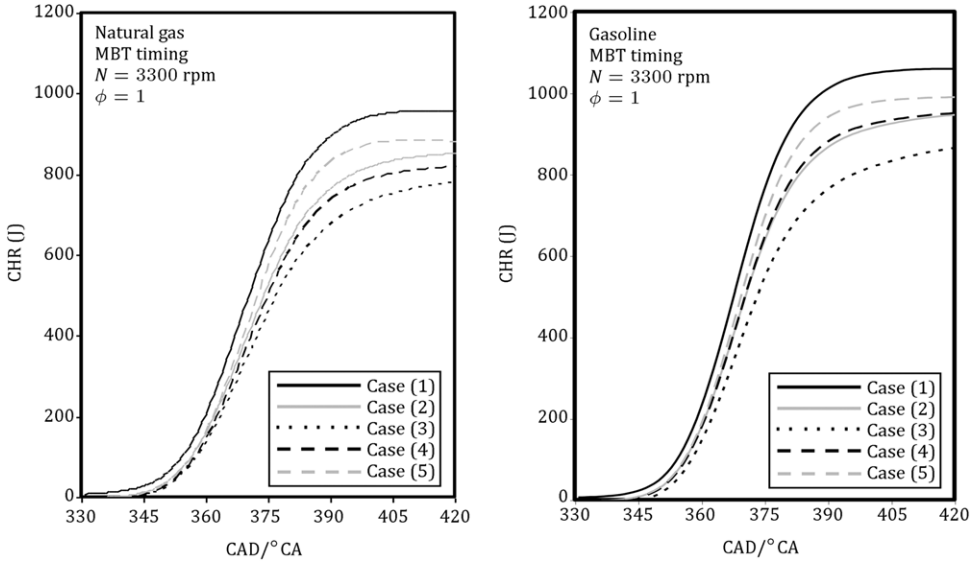

Figure 4: Sensitivity of CHR for cases 1–5.

Figures 4 and 3, it is obvious that the effect of varying the specific heat ratio on the trend of variation of the CHR curve and on the trend of variation of the HRR curve is similar.

6.3. Mass fraction burned

Combustion starts almost immediately after spark ignition, but as the first stages are quite slow, combustion beginning is used to describe the start of combustion. It is quite difficult to precisely determine the end of combustion, due to the late burning phenomenon [18]. For these reasons, combustion beginnings and ends are arbitrarily defined. The variations of 10% MFBP and 90% MFBP for five cases are plotted in Figure 5. The 10% MFBP takes place earlier, with respect to the Top Dead Center (TDC) in case1, followed by cases 2, 5, 4 and 3 for both fuels. The 90% MFBP is found earlier, with respect to TDC in case 1 for both fuels, followed by cases 5, 4, 2 and 3 for gasoline operation, and cases 5, 2, 4 and 3 for natural gas operation. The average SD of 10% MFBP and 90% MFBP between cases 1–3 are about 1.5 and 5.7 °CA for natural gas operation, and about 1.3 and 8.5 °CA for gasoline operation, respectively. It means that 10% MFBP of natural gas operation is more sensitive to specific heat ratio variation than that of gasoline operation, while 90% MFBP of gasoline operation is more sensitive to specific heat ratio variation. It is due to the fact that the value of 10% MFB at natural gas operation is higher than that of gasoline operation, but after around 20% MFB, the value of MFB at gasoline operation is higher than that of gasoline operation for cases 1–3. It is also found that the average SD of 10% and 90% MFBP between cases 4 and 5, for natural gas operation, are about 44.2% and 9% higher, respectively, than that for gasoline operation. It means that 10% and 90% MFBP of natural gas operation are more sensitive to the first derivative of the specific heat ratio, than that of gasoline operation.

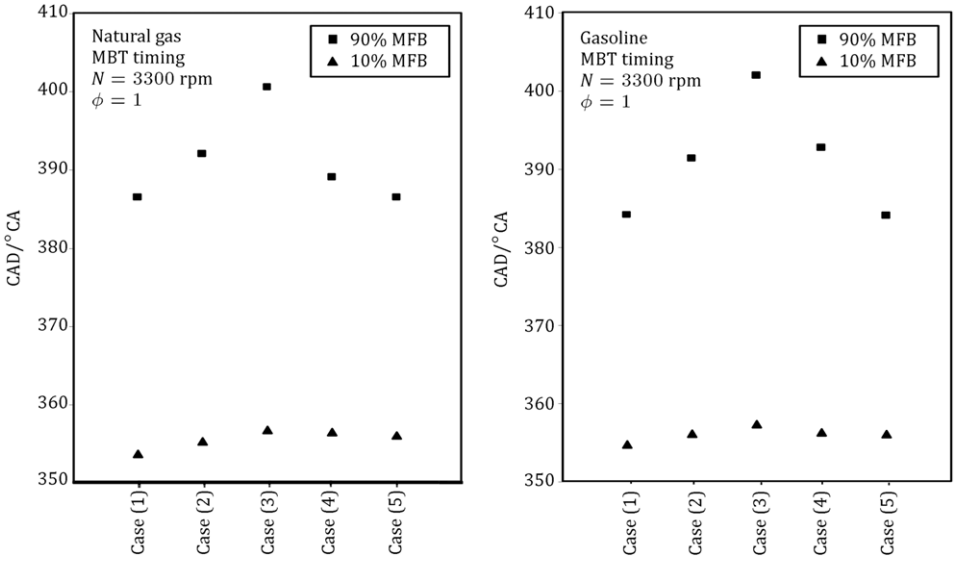

Figure 5: Sensitivity of 10% MFBP and 90% MFBP for cases 1–5.

7. Conclusion

In this work, the effects of assumed specific heat ratio on the heat release analysis of engine pressure data are studied by applying the first law of thermodynamics to the cylinder charge, which is assumed to be an ideal gas mixture. The tests were carried out with the spark timing adjusted to MBT timing at an equivalence ratio of $\phi = 1$, and speed engine of $N = 3300$ rpm, for gasoline and natural gas operations.

The following conclusions were drawn from the results:

- A low value of specific heat ratio causes an increase in the magnitude and shape of HRR and CHR curves.
- The combustion parameters for natural gas operation are more sensitive to the first derivative of the specific heat ratio than that for gasoline operation.
- The effect of various specific heat ratios, from 1.25 to 1.35 on HRR, CHR, CHR_{max} and 90% MFBP for gasoline operation, is higher than that for natural gas operation, while the effect of various specific heat ratios on HRR/HRR_{max} and 10% MFBP for natural gas operation is higher.

References

[1] Tiourad, M. and Mozafari, A. "Prediction of stratified charge divided chamber engine performance", *Sci. Iran. Trans. B: Mech. Eng.*, 16(1), pp. 92–100 (2009).
[2] Klein, M. "A specific heat ratio model and compression ratio estimation", Ph.D. Thesis, Department of Electrical Engineering, Linkoping University, Sweden (2004).
[3] Ebrahimi, R. and Desmet, B. "An experimental investigation on engine speed and cyclic dispersion in an HCCI engine", *Fuel*, 89(8), pp. 2149–2156 (2010).
[4] Fathi, M., Saray, R.Kh. and Checkel, M.D. "Detailed approach for apparent heat release analysis in HCCI engines", *Fuel*, 89(9), pp. 2323–2330 (2010).
[5] Abu-Nada, E., Al-Hinti, I., Al-Sarkhi, A. and Akash, B. "Thermodynamic modeling of spark-ignition engine: effect of temperature dependent specific heats", *Int. Commun. Heat Mass Transfer*, 33, pp. 1264–1272 (2006).
[6] Klein, M. and Erikson, L. "A specific heat ratio model for single-zone heat release models", SAE paper 2004-01-1464 (2004).
[7] Lanzafame, R. and Messina, M. "ICE gross heat release strongly influenced by specific heat ratio values", *Int. J. Automotive Technol.*, 4(3), pp. 125–133 (2003).
[8] Brunt, M.F.J., Rai, H. and Emtage, A.L. "The calculation of heat release energy from engine cylinder pressure data", SAE paper 981052 (1998).
[9] Chun, K.M. and Heywood, J.B. "Estimated heat-release and mass-of-mixture burned from spark-ignition engine pressure data", *Combust. Sci. Technol.*, 54, pp. 133–143 (1987).
[10] Espey, C. and Dec, J.E. "The effect of TDC temperature and density on the liquid-phase fuel penetration in a D.I. Diesel engine", SAE paper 952456 (1995).
[11] Holman, J.P., *Experimental Methods for Engineers*, 5th ed. McGraw Hill, New York (1989).
[12] Ferguson, C.R., *Internal Combustion Engines, Applied Thermosciences*, 2nd ed. John Wiley & Sons, New York (2001).
[13] Ceviz, M.A. and Kaymaz, I. "Temperature and air–fuel ratio dependent specific heat ratio functions for lean burned and unburned mixture", *Energy Convers. Manage.*, 46, pp. 2387–2404 (2005).
[14] Olikara, C. and Borman, G. "A computer program for calculating properties of equilibrium combustion products with some applications on IC engines", SAE Paper 750468 (1975).
[15] Sameca, N., Kegla, B. and Dibble, R.W. "Numerical and experimental study of water/oil emulsified fuel combustion in a diesel engine", *Fuel*, 81, pp. 2035–2044 (2002).
[16] Shudo, T. and Suzuki, H. "Applicability of heat transfer equations to hydrogen combustion", *JSAE Rev.*, 23, pp. 303–308 (2002).
[17] Woschni, G. "A universally applicable equation for the instantaneous heat transfer coefficient in the internal combustion engine", SAE Paper 670931 (1967).
[18] Zervas, E. "Comparative study of some experimental methods to characterize the combustion process in a SI engine", *Energy*, 30, pp. 1803–1816 (2005).

Rahim Ebrahimi is Assistant Professor at the Department of Agriculture Machine Mechanics, Shahrekord University, Iran. He received his Ph.D. in Mechanical Engineering from Université de Valenciennes et du Hainaut Cambrésis, France, in 2006. He is actively involved in teaching and research activities in the field of internal combustion engines and finite-time thermodynamic analysis of heat engines. He has authored many papers in international journals, and for national and international conferences.